

# FOURTH ORDER TIME-STEPPING FOR KADOMTSEV-PETVIASHVILI AND DAVEY-STEWARTSON EQUATIONS\*

C. KLEIN<sup>†</sup> AND K. ROIDOT<sup>‡</sup>

**Abstract.** Purely dispersive partial differential equations as the Korteweg-de Vries equation, the nonlinear Schrödinger equation and higher dimensional generalizations thereof can have solutions which develop a zone of rapid modulated oscillations in the region where the corresponding dispersionless equations have shocks or blow-up. To numerically study such phenomena, fourth order time-stepping in combination with spectral methods is beneficial to resolve the steep gradients in the oscillatory region. We compare the performance of several fourth order methods for the Kadomtsev-Petviashvili and the Davey-Stewartson equations, two integrable equations in 2+1 dimensions: exponential time-differencing, integrating factors, time-splitting, implicit Runge-Kutta and Driscoll's composite Runge-Kutta method. The accuracy in the numerical conservation of integrals of motion is discussed.

**Key words.** Exponential time-differencing, Kadomtsev-Petviashvili equation, Davey-Stewartson systems, split step, integrating factor method, dispersive shocks

**AMS subject classifications.** Primary, 65M70; Secondary, 65L05, 65M20

**1. Introduction.** Nonlinear dispersive partial differential equations (PDEs) play an important role in applications since they appear in many approximations to systems in hydrodynamics, nonlinear optics, acoustics, plasma physics, Bose-Einstein condensates among others. The most prominent members of the class are the celebrated Korteweg-de Vries (KdV) equation and the nonlinear Schrödinger (NLS) equation and higher dimensional generalizations of these. In addition to the importance of these equations in applications, there is also a considerable interest in the mathematical properties of their solutions. It is known that nonlinear dispersive PDEs without dissipation can have *dispersive shock waves* [?], i.e., regions of rapid modulated oscillations in the vicinity of shocks in the solutions to the corresponding dispersionless equations for the same initial data. Thus solutions to dispersive PDEs in general will not have a strong dispersionless limit as known from solutions to dissipative PDEs as the Burgers' equation in the limit of vanishing dissipation. An asymptotic description of these dispersive shocks is known for certain integrable PDEs as KdV [?, ?, ?] and the NLS equation for certain classes of initial data [?, ?, ?]. For KdV an example is shown in Fig. 1.1, for details see [?].

No such description is known for  $2 + 1$ -dimensional PDEs. In addition solutions to nonlinear dispersive PDEs can have *blowup*, i.e., in finite time a loss of regularity of the solution with respect to the initial data. It is known for many of the PDEs under consideration when blowup can occur, but for the precise mechanism of the blowup often not even conjectures exist.

---

\*We thank P. Matthews, B. Muite, A. Ostermann, T. Schmelzer, who provided example codes, and L.N. Trefethen, who interested us in the subject, for helpful discussion and hints. This work has been supported by the project FroM-PDE funded by the European Research Council through the Advanced Investigator Grant Scheme, the Conseil Régional de Bourgogne via a FABER grant and the ANR via the program ANR-09-BLAN-0117-01.

<sup>†</sup>Institut de Mathématiques de Bourgogne, Université de Bourgogne, 9 avenue Alain Savary, 21078 Dijon Cedex, France ([christian.klein@u-bourgogne.fr](mailto:christian.klein@u-bourgogne.fr))

<sup>‡</sup>Institut de Mathématiques de Bourgogne, Université de Bourgogne, 9 avenue Alain Savary, 21078 Dijon Cedex, France ([kristelle.roidot@u-bourgogne.fr](mailto:kristelle.roidot@u-bourgogne.fr))

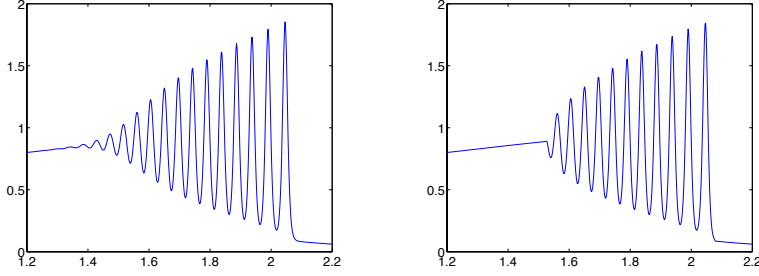


FIG. 1.1. Numerical solution of KdV for the initial data  $u_0(x) = 1/\cosh^2 x$  (left) and the corresponding asymptotic solution (right) for  $t = 0.35$  and  $\epsilon = 10^{-2}$  (see [?]).

In view of the importance of the equations and the open mathematical questions, efficient numerical algorithms are needed to enable extensive numerical studies of the PDEs. The focus of the present work is to study a  $2+1$ -dimensional generalization of the KdV equation, the Kadomtsev-Petviashvili (KP) equation, and a  $2+1$ -dimensional generalization of the NLS equation, the Davey-Stewartson (DS) equation. The former takes the form

$$\partial_x (\partial_t u + 6u\partial_x u + \epsilon^2 \partial_{xxx} u) + \lambda \partial_{yy} u = 0, \quad \lambda = \pm 1 \quad (1.1)$$

where  $(x, y, t) \in \mathbb{R}_x \times \mathbb{R}_y \times \mathbb{R}_t$  and where  $\epsilon \ll 1$  is a small scaling parameter. The limit  $\epsilon \rightarrow 0$  is the dispersionless limit. The case  $\lambda = -1$  corresponds to the KP I model with a *focusing* effect, and the case  $\lambda = 1$  corresponds to the KP II model with a *defocusing* effect. The former is also known as the *unstable* KP equation since the soliton solution of the KdV equation is linearly unstable for KP I, whereas it is linearly stable for the latter, which is therefore also known as the *stable* KP equation. These stability issues were numerically studied in [?]. It is an interesting result of the present paper that both KP equations have very similar numerical convergence properties despite completely different stability properties of their exact solutions in [?]. These equations appear in different fields of physics in the study of essentially one-dimensional wave phenomena with weak transverse effects, for example to model nonlinear dispersive waves on the surface of fluids [?]. In this case, KP I is used when the surface tension is strong, and KP II when the surface tension is weak. They also model sound waves in ferromagnetic media [?], and nonlinear matter-wave pulses in Bose-Einstein condensates [?]. The KP equation was introduced by Kadomtsev and Petviashvili in [?] to study the stability of the KdV soliton against weak transverse perturbations. It was shown to be completely integrable in [?]. Higher dimensional generalizations of the KP equations, where the derivative  $\partial_{yy}$  is replaced by the Laplacian in the transverse coordinates,  $\Delta^\perp = \partial_{yy} + \partial_{zz}$ , are important for instance in acoustics. The numerical problems to be expected there are the same as in the  $2+1$ -dimensional case studied here.

The Davey-Stewartson system can be written in the form

$$\begin{aligned} i\epsilon \partial_t u + \epsilon^2 \partial_{xx} u - \alpha \epsilon^2 \partial_{yy} u + 2\rho (\Phi + |u|^2) u &= 0, \\ \partial_{xx} \Phi + \beta \partial_{yy} \Phi + 2\partial_{xx} |u|^2 &= 0, \end{aligned} \quad (1.2)$$

where  $\alpha$ ,  $\beta$  and  $\rho$  take the values  $\pm 1$ , where  $\epsilon \ll 1$  is again a small dispersion pa-

parameter, and where  $\Phi$  is a mean field. Since the  $\epsilon$  has the same role as the  $\hbar$  in the Schrödinger equation, the limit  $\epsilon \rightarrow 0$  is also called the semiclassical limit in this context. The DS equations are classified [?] according to the ellipticity or hyperbolicity of the operators in the first and second line. The case  $\alpha = \beta$  is completely integrable [?] and thus provides a  $2 + 1$ -dimensional generalization of the integrable NLS equation in  $1 + 1$  dimensions. The integrable cases are elliptic-hyperbolic called DS I, and the hyperbolic-elliptic called DS II. For both there is a focusing ( $\rho = -1$ ) and a defocusing ( $\rho = 1$ ) version. In the following, we will only consider the case DS II ( $\alpha = 1$ ) since the mean field  $\Phi$  is then obtained by inverting an elliptic operator. These DS systems model the evolution of weakly nonlinear water waves that travel predominantly in one direction, but in which the wave amplitude is modulated slowly in two horizontal directions [?], [?]. They are also used in plasma physics [?, ?], to describe the evolution of a plasma under the action of a magnetic field.

Since both KP and DS are completely integrable, there exist many explicit solutions, which thus provide popular test cases for numerical algorithms. But as we will show for the example of KP, these exact solutions, typically solitons, often test the equation in a regime where stiffness is not important. The main challenge in the study of critical phenomena as dispersive shocks and blowups is, however, the numerical resolution of strong gradients in the presence of which the above equations are very stiff. This implies that algorithms that perform well for solitons might not be efficient in the context studied here.

Since critical phenomena are generally believed to be independent of the chosen boundary conditions, we study a periodic setting<sup>1</sup>. Such settings also include rapidly decreasing functions which can be periodically continued as smooth functions within the finite numerical precision. This allows one to approximate the spatial dependence via truncated Fourier series which leads for the studied equations to large stiff systems of ODEs, see below. The use of Fourier methods not only gives spectral accuracy in the spatial coordinates, but also minimizes the introduction of numerical dissipation which is important in the study of dispersive effects. In Fourier space, equations (1.1) and (1.2) have the form

$$v_t = \mathbf{L}v + \mathbf{N}(v, t), \quad (1.3)$$

where  $v$  denotes the (discrete) Fourier transform of  $u$ , and where  $\mathbf{L}$  and  $\mathbf{N}$  denote linear and nonlinear operators, respectively. The resulting systems of ODEs are classical examples of stiff equations where the stiffness is related to the linear part  $\mathbf{L}$  (it is a consequence of the distribution of the eigenvalues of  $\mathbf{L}$ ), whereas the nonlinear part contains only low order derivatives. In the small dispersion limit, this stiffness is still present despite the small term  $\epsilon^2$  in  $\mathbf{L}$ . This is due to the fact that the smaller  $\epsilon$  is, the higher wavenumbers are needed to resolve the rapid oscillations. The first numerical studies of exact solutions to the KP equations were performed in [?] and [?] and references therein. For the DS system similar studies were done in [?]. In [?] blowup for DS was studied for the analytically known blowup solution by Ozawa [?].

There are several approaches to deal efficiently with equations of the form (1.3) with a linear stiff part, implicit-explicit (IMEX), time splitting, integrating factor (IF), and deferred correction schemes as well as sliders and exponential time differencing. To avoid as much as possible a pollution of the Fourier coefficients by errors due to the finite difference schemes for the time integration and to allow the use of

---

<sup>1</sup>The boundary conditions will, however, in general influence convergence of the used numerical schemes. The restriction in this paper to periodic conditions is due to the studied problems.

larger time steps, we mainly consider fourth order schemes. While standard explicit schemes impose prohibitively small time steps due to stability requirements (for the studied examples the standard fourth order Runge-Kutta (RK) scheme did not converge for the used time steps), stable implicit schemes are in general computationally too expensive in  $2+1$  dimensions. As an example of the latter we consider an implicit fourth order Runge-Kutta scheme. The focus of this paper is, however, to compare the performance of several explicit fourth order schemes mainly related to exponential integrators for various examples in a similar way as in the work by Kassam and Trefethen [?] and in [?] for KdV and NLS.

The paper is organized as follows: In section 2 we briefly list the used numerical schemes, integrating factor methods, exponential time differencing, lineary implicit schemes, time splitting methods and implicit Runge-Kutta schemes. In section 3 we review some analytical facts for the KP equations and study for each of the equations an exact solution and an example in the small dispersion limit. In section 4 a similar analysis is presented for the semiclassical limit of the focusing and the defocusing DS II equation. The found numerical errors are compared in section 5 with the error indicated by a violation of the conservation of the  $L_2$  norm by the numerical solution. In section 6 we add some concluding remarks and outline further directions of research.

**2. Numerical Methods.** In this paper we are mainly interested in the numerical study of the KP and the DS II equations for Schwartzian initial data in the small dispersion limit. The latter implies that we can treat the problem as essentially periodic, and that we can use Fourier methods. After spatial discretization we thus face a system of ODEs of the form (1.3). Since we need to resolve high wavenumbers, these systems will be in general rather large. The PDEs studied here have high order derivatives in the linear part  $\mathbf{L}$  of (1.3), whereas the nonlinear part  $\mathbf{N}$  contains only first derivatives. This means that the stiffness in these systems is due to the linear part. The latter will thus be treated with adapted methods detailed below, whereas standard methods can be used for the nonlinear part. We restrict the analysis to moderate values of the dispersion parameter to be able to study the dependence of the different schemes on the time step in finite CPU time. For smaller values of  $\epsilon$  see for instance [?].

We will compare several numerical schemes for equations of the form (1.3) as in [?] and [?]. The PDEs are studied for a periodic setting with periods  $2\pi L_x$  and  $2\pi L_y$  in  $x$  and  $y$  respectively. We give the numerical error in dependence of the number  $N_t$  of time steps as well as the actual CPU time as measured by MATLAB (all computations are done on a machine with Intel ‘Nehalem’ processors with 2.93 GHz with codes in MATLAB 7.10). The goal is to provide some indication on the actual performance of the codes in practical applications. Since MATLAB is using in general a mixture of interpreted and precompiled embedded code, a comparison of computing times is not unproblematic. However, it can be done in the present context since the main computational cost is due to two-dimensional fast Fourier transformations (FFT). For the KP equations all considered approaches (with the exception of the Hochbruck-Ostermann ETD scheme which uses 8 FFT commands per time step) use 6 (embedded) FFT commands per time step as was already pointed out in [?]. For the DS II equation, these numbers are doubled since the computation of the mean field  $\Phi$  takes another FFT/IFFT pair per intermediate step. Note that an additional FFT/IFFT pair per time step is needed in both cases to switch between physical and Fourier space (we are interested in a solution in physical space, but the schemes are formulated for the Fourier transforms). The  $\phi$ -functions in the ETD schemes are

also computed via FFT. It can be seen that this can be done with machine precision in a very efficient way. Since the  $\phi$ -functions have to be obtained only once in the computation and since the studied problems are computationally demanding, this only has a negligible effect on the total CPU time in the experiments. The numerical error is the  $L_2$  norm of the difference of the numerical solution and an exact or reference solution, normalized by the  $L_2$  norm of the initial data. It is denoted by  $\Delta_2$ .

**2.1. Integrating Factor Methods (IF).** These methods appeared first in the work of Lawson [?], see [?] for a review. He suggested to take care of the stiff linear part of equation (1.3) by using a change of the dependent variables (also called the Lawson transformation)  $w(t) = e^{-\mathbf{L}t}v(t)$ . Equation (1.3) becomes

$$w'(t) = e^{-\mathbf{L}t}\mathbf{N}(v, t) \quad (2.1)$$

for which we use a fourth order Runge-Kutta (RK) scheme. Hochbruck and Ostermann [?] showed that this IF method has classical order four, but not what they call *stiff order* four. Loosely speaking there can be additional contributions to the error of much lower order in the time step due to the stiffness, i.e., in the case of large norm  $\|\mathbf{L}\|$  in the integrating factor. They could show that the scheme used here can reduce to first order for semilinear parabolic problems. The Hochbruck-Ostermann approach uses semigroups. An extension of their theory to hyperbolic equations is possible via  $C_0$  semigroups, which can lead, however, to a slightly lower order of convergence. But the results in [?], [?] indicate that similar convergence rates are to be expected for hyperbolic equations (both KP and DS are hyperbolic in the sense that the matrix  $\mathbf{L}$  appearing in (1.3) has purely imaginary eigenvalues).

**2.2. Driscoll's composite Runge-Kutta Method.** The idea of IMEX methods (see e.g. [?] for KdV) is the use of a stable implicit method for the linear part of the equation (1.3) and an explicit scheme for the nonlinear part which is assumed to be non-stiff. In [?] such schemes did not perform satisfactorily for dispersive PDEs which is why we only consider a more sophisticated variant here. Fornberg and Driscoll [?] provided an interesting generalization of IMEX by splitting also the linear part of the equation in Fourier space into regimes of high, medium, and low wavenumbers, and by using adapted numerical schemes in each of them. They considered the NLS equation as an example. Driscoll's [?] idea was to split the linear part of the equation in Fourier space just into regimes of high and low wavenumbers. He used the fourth order RK integrator for the low wavenumbers and the lineary implicit RK method of order three for the high wavenumbers. He showed that this method is in practice of fourth order over a wide range of step sizes. We confirm this here for the cases where the method converges, which it fails to do, however, sometimes for very stiff problems. In particular, he used this method for the KP II equation at the two phase solution we will also discuss in this paper as a test case. We call the method DCRK in the following.

**2.3. Exponential Time Differencing Methods.** Exponential time differencing schemes were developed originally by Certainé [?] in the 60s, see [?] and [?] for comprehensive reviews of ETD methods and their history. The basic idea is to use equidistant time steps  $h$  and to integrate equation (1.3) exactly between the time steps  $t_n$  and  $t_{n+1}$  with respect to  $t$ . With  $v(t_n) = v_n$  and  $v(t_{n+1}) = v_{n+1}$ , we get

$$v_{n+1} = e^{\mathbf{L}h}v_n + \int_0^h e^{\mathbf{L}(h-\tau)}\mathbf{N}(v(t_n + \tau), t_n + \tau)d\tau.$$

The integral will be computed in an approximate way for which different schemes exist. We use here only Runge-Kutta schemes of classical order 4, Cox-Matthews [?], Krogstad [?] and Hochbruck-Ostermann [?]. The latter showed that the stiff order of the Cox-Matthews scheme is only two, and the one of Krogstad's is three. Notice that both schemes can be of stiff order four if the studied system satisfies a certain number of non-trivial auxiliary conditions, see [?]. As the numerical tests show in the following, order reduction can be observed in some cases, but not in all. We will speak in the following of the *stiff regime* of an equation where order reduction can be observed, or where certain schemes do not converge, and of the *non-stiff regime*, where this is not the case. Note that this is not a rigorous definition. Both Cox-Matthews' and Krogstad's schemes are, however, four-stage methods, whereas the Hochbruck-Ostermann method is a five-stage method that has stiff order four. Thus all these methods should show the same convergence rate in the non-stiff regime, but could differ for some problems in the stiff regime. Notice that these results [?] were established for parabolic PDEs, and that the applicability for hyperbolic PDEs of the type studied here is not obvious. One of the purposes of our study is to get some experimental insight whether the Hochbruck-Ostermann theory holds also in this case.

The main technical problem in the use of ETD schemes is the efficient and accurate numerical evaluation of the functions

$$\phi_i(z) = \frac{1}{(i-1)!} \int_0^1 e^{(1-\tau)z} \tau^{i-1} d\tau, \quad i = 1, 2, 3, 4,$$

i.e., functions of the form  $(e^z - 1)/z$  and higher order generalizations thereof, where one has to avoid cancellation errors. Kassam and Trefethen [?] used complex contour integrals to compute these functions. The approach is straight forward for diagonal operators  $\mathbf{L}$  that occur here because of the use of Fourier methods: one considers a unit circle around each point  $z$  and computes the contour integral with the trapezoidal rule which is known to be a spectral method in this case. Schmelzer [?] made this approach more efficient by using the complex contour approach only for values of  $z$  close to the pole, e.g with  $|z| < 1/2$ . For the same values of  $z$  the functions  $\phi_i$  can be computed via a Taylor series. These two independent and very efficient approaches allow a control of the accuracy. We find that just 16 Fourier modes in the computation of the complex contour integral are sufficient to determine the functions  $\phi_i$  to the order of machine precision. Thus we avoid problems reported in [?], where machine precision could not be reached by ETD schemes due to inaccuracies in the determination of the  $\phi$ -functions. The computation of these functions takes only negligible time for the  $2 + 1$ -dimensional equations studied here, especially since it has to be done only once during the time evolution. We find that ETD as implemented in this way has the same computational costs as the other used schemes.

**2.4. Splitting Methods.** Splitting methods are convenient if an equation can be split into two or more equations which can be directly integrated. The motivation for these methods is the Trotter-Kato formula [?, ?]

$$\lim_{n \rightarrow \infty} \left( e^{-tA/n} e^{-tB/n} \right)^n = e^{-t(A+B)} \quad (2.2)$$

where  $A$  and  $B$  are certain unbounded linear operators, for details see [?]. In particular this includes the cases studied by Bagrinovskii and Godunov in [?] and by Strang [?]. For hyperbolic equations, first references are Tappert [?] and Hardin and Tappert [?] who introduced the split step method for the NLS equation.

The idea of these methods for an equation of the form  $u_t = (A + B)u$  is to write the solution in the form

$$u(t) = \exp(c_1 t A) \exp(d_1 t B) \exp(c_2 t A) \exp(d_2 t B) \cdots \exp(c_k t A) \exp(d_k t B) u(0)$$

where  $(c_1, \dots, c_k)$  and  $(d_1, \dots, d_k)$  are sets of real numbers that represent fractional time steps. Yoshida [?] gave an approach which produces split step methods of any even order.

The KP equation can be split into

$$u_t + 6uu_x = 0, \quad (2.3)$$

$$(\mathcal{F}[u])_t - ik_x^3 \mathcal{F}[u] + \lambda \frac{ik_y^2}{k_x} \mathcal{F}[u] = 0, \quad (2.4)$$

where here and in the following we write the 2-dimensional Fourier transform of  $u$  in the form

$$\mathcal{F}[u] := \int_{\mathbb{R}^2} u(x, y, t) e^{-ik_x x - ik_y y} dx dy. \quad (2.5)$$

The Hopf equation (2.3) can be integrated in implicit form with the method of characteristics, and the linear equation in Fourier space (2.4) can be directly integrated, but the implicit form of the solution of the former makes an iteration with interpolation to the characteristic coordinates necessary that is computationally too expensive. Therefore we consider splitting here only for the DS equation. The latter can be split into

$$i\epsilon u_t = \epsilon^2(-u_{xx} + \alpha u_{yy}), \quad \Phi_{xx} + \alpha \Phi_{yy} + 2(|u|^2)_{xx} = 0, \quad (2.6)$$

$$i\epsilon u_t = -2\rho \left( \Phi + |u|^2 \right) u, \quad (2.7)$$

which are explicitly integrable, the first two in Fourier space, equation (2.7) in physical space since  $|u|^2$  is a constant in time for this equation. Convergence of second order splitting along these lines was studied in [?]. We study here second and fourth order splitting schemes for DS as given in [?].

**2.5. Implicit Runge Kutta Scheme.** The general formulation of an  $s$ -stage Runge–Kutta method for the initial value problem  $y' = f(y, t)$ ,  $y(t_0) = y_0$  is the following:

$$y_{n+1} = y_n + h \sum_{i=1}^s b_i K_i, \quad (2.8)$$

$$K_i = f \left( t_n + c_i h, y_n + h \sum_{j=1}^s a_{ij} K_j \right), \quad (2.9)$$

where  $b_i$ ,  $a_{ij}$ ,  $i, j = 1, \dots, s$  are real numbers and  $c_i = \sum_{j=1}^s a_{ij}$ .

For the implicit Runge–Kutta scheme of order 4 (IRK4) used here (Hammer–Hollingsworth method), we have  $c_1 = \frac{1}{2} - \frac{\sqrt{3}}{6}$ ,  $c_2 = \frac{1}{2} + \frac{\sqrt{3}}{6}$ ,  $a_{11} = a_{22} = 1/4$ ,  $a_{12} = \frac{1}{4} - \frac{\sqrt{3}}{6}$ ,  $a_{21} = \frac{1}{4} + \frac{\sqrt{3}}{6}$  and  $b_1 = b_2 = 1/2$ . This scheme is also known as the

2-stage Gauss method. It is of classical order 4, but stage order 2. This is the reason why an order reduction to second order can be observed in certain examples.

The implicit character of this method requires the iterative solution of a high dimensional system at every step which is done via a simplified Newton method. For the studied examples in the form (1.3), we have to solve equations of the form

$$y = \mathbf{A}y + b(y)$$

for  $y$ , where  $\mathbf{A}$  is a linear operator independent of  $y$ , and where  $b$  is a vector with a nonlinear dependence on  $y$ . These are solved iteratively in the form

$$y_{n+1} = (1 - \mathbf{A})^{-1}b(y_n).$$

By treating the linear part that is responsible for the stiffness explicitly as in an IMEX scheme, the iteration converges in general quickly. Without taking explicit care of the linear part, convergence will be extremely slow. The iteration is stopped once the  $L_\infty$  norm of the difference between consecutive iterates is smaller than some threshold (in practice we work with a threshold of  $10^{-8}$ ). Per iteration the computational cost is essentially 2 FFT/IFFT pairs. Thus the IRK4 scheme can be competitive with the above explicit methods which take 3 or 4 FFT/IFFT pairs per time step if not more than 2-3 iterations are needed per time step. This can happen in the below examples in the non-stiff regime, but is not the case in the stiff regime. We only test this scheme where its inclusion appears interesting and where it is computationally not too expensive.

**3. Kadomtsev-Petviashvili Equation.** In this section we study the efficiency of the above mentioned numerical schemes in solving Cauchy problems for the KP equations. We first review some analytic facts about KP I and KP II which are important in this context. Since the KP equations are completely integrable, exact solutions exist that can be used as test cases for the codes. We compare the performance of the codes for the exact solutions and a typical example in the small dispersion limit.

**3.1. Analytic Properties of the KP Equations.** We will collect here some analytic aspects of the KP equations which will be important for an understanding of several issues in the numerical solution of Cauchy problems for the KP equations, see [?] for a recent review and references therein.

In this paper we will look for KP solutions that are periodic in  $x$  and  $y$ , i.e., for solutions on  $\mathbb{T}^2 \times \mathbb{R}$ . This includes for numerical purposes the case of rapidly decreasing functions in the Schwartz space  $\mathcal{S}(\mathbb{R}^2)$  if the periods are chosen large enough that  $|u|$  is smaller than machine precision (we work with double precision throughout the article) at the boundaries of the computational domain. Notice, however, that solutions to Cauchy problems with Schwartzian initial data  $u_0(x, y)$  will not stay in  $\mathcal{S}(\mathbb{R}^2)$  unless  $u_0(x, y)$  satisfies an infinite number of constraints. This behaviour can be already seen on the level of the linearized KP equation, see e.g. [?, ?], where the Green's function implies a slow algebraic decrease in  $y$  towards infinity. This leads to the formation of *tails* with an algebraic decrease to infinity for generic Schwartzian initial data. The amplitude of these effects grows with time (see for instance [?]). In our periodic setting this will give rise to *echoes* and a weak Gibbs phenomenon at the boundaries of the computational domain. The latter implies that we cannot easily reach machine precision as in the KdV case unless we use considerably larger domains. As can be seen from computations in the small dispersion limit below and the Fourier coefficients in sect. 5, we can nonetheless reach an accuracy of better than  $10^{-10}$  on



the chosen domain. For higher precisions and larger values of  $t$ , the Gibbs phenomena due to the algebraic tails become important.

The KP equation (1.1) is not in the standard form for a Cauchy problem. As discussed in [?]  $t$  is not a timelike but characteristic coordinate if the dispersionless KP equation ( $\epsilon = 0$ ) is considered as a standard second order PDE. In practice one is, however, interested in the Cauchy problem for  $t$ . To this end one writes (1.1) in *evolutionary form*

$$\partial_t u + 6u\partial_x u + \epsilon^2 \partial_{xxx} u = -\lambda \partial_x^{-1} \partial_{yy} u, \quad \lambda = \pm 1. \quad (3.1)$$

Equations (3.1) and (1.1) are equivalent for certain classes of boundary conditions as periodic or rapidly decreasing at infinity. Since we will always impose periodic boundary conditions in the following, both forms of the KP equation are equivalent for our purposes. The antiderivative  $\partial_x^{-1}$  is to be understood as the Fourier multiplier with the singular symbol  $-i/k_x$ . In the numerical computation this multiplier is regularized in standard way (similar to the Dirac regularization of  $1/x$  by adding an arbitrary small imaginary part  $i0$  to  $x$ ) as

$$\frac{-i}{k_x + i\lambda\delta},$$

where we choose  $\delta = \text{eps} = 2^{-52} \sim 2.2 * 10^{-16}$ . Since the typical precision to be achieved in the studied examples with double precision is of the order  $10^{-14}$  because of rounding errors, this is essentially equivalent to adding a numerical zero (see also the discussion in [?]).

The divergence structure of the KP equations has the consequence that

$$\int_{\mathbb{T}} \partial_{yy} u(x, y, t) dx = 0, \quad \forall t > 0, \quad (3.2)$$

even if this constraint is not satisfied for the initial data  $u_0(x, y)$ . It was shown in [?, ?] that the solution to a Cauchy problem not satisfying the constraint will not be smooth in time for  $t = 0$ . Numerical experiments in [?] indicate that the solution after an arbitrary small time step will develop an infinite ‘trench’ the integral over which just ensures that (3.2) is fulfilled. To propagate such initial data, the above regularization is in fact needed (for data satisfying the constraint via the condition that the Fourier coefficients for  $k_x = 0$  vanish, this property could be just imposed at each time step). The infinite trench due to initial data not satisfying the constraint implies a rather strong Gibbs phenomenon. To avoid the related problems, we always consider initial data that satisfy (3.2). A possible way to achieve this is to consider data that are  $x$ -derivatives of periodic or Schwartzian functions.

The complete integrability of the KP equations implies that efficient tools exist for the generation of exact solutions. We always put  $\epsilon = 1$  for the exact solutions. For a recent review of the integrable aspects of KP see [?]. The most popular KP solutions are *line solitons*, i.e., solutions localized in one spatial direction and infinitely extended in another. Such solutions typically have an angle not equal to 0 or 90 degrees with the boundaries of the computational domain, which leads to strong Gibbs phenomena. This implies that these solutions are not a good test case for a periodic setting. If the angle is 0 or 90 degrees, the solution only depends on one of the spatial variables and thus does not test a true 2d code. There exists a *lump* soliton for KP I which is localized in all spatial directions, but only with algebraic fall off. This would again lead to strong Gibbs phenomena in our setting.

However a solution due to Zaitsev [?] to the KP I equation is localized in one direction and periodic in the second (a transformation of the form  $x \rightarrow ix$ ,  $y \rightarrow iy$  exchanges these two directions). It has the form

$$u(\xi, y) = 2\alpha^2 \frac{1 - \beta \cosh(\alpha\xi) \cos(\delta y)}{(\cosh(\alpha\xi) - \beta \cos(\delta y))^2} \quad (3.3)$$

where

$$\xi = x - ct, \quad c = \alpha^2 \frac{4 - \beta^2}{1 - \beta^2}, \quad \text{and} \quad \delta = \sqrt{\frac{3}{1 - \beta^2}} \alpha^2.$$

This solution is localized in  $x$ , periodic in  $y$ , and unstable as discussed in [?].

Algebro-geometric solutions to the KP equation can be constructed on an arbitrary compact Riemann surface, see e.g. [?], [?]. These solutions are in general almost periodic. Solutions on genus 2 surfaces, which are all hyperelliptic, are exactly periodic, but in general not in both  $x$  and  $y$ . A doubly periodic solution with exactly this property of KP II of genus 2 can be written as

$$u(x, y, t) = 2 \frac{\partial^2}{\partial x^2} \ln \theta(\varphi_1, \varphi_2; B) \quad (3.4)$$

where  $\theta(\varphi_1, \varphi_2; B)$  is defined by the double Fourier series

$$\theta(\varphi_1, \varphi_2; B) = \sum_{m_1=-\infty}^{\infty} \sum_{m_2=-\infty}^{\infty} e^{\frac{1}{2} m^T B m + i m^T \varphi} \quad (3.5)$$

where  $m^T = (m_1, m_2)$ , and where  $B$  is a  $2 \times 2$  symmetric, negative-definite Riemann matrix

$$B = \begin{pmatrix} b & b\lambda \\ b\lambda & b\lambda^2 + d \end{pmatrix}, \quad \text{with real parameters } \lambda \neq 0, b \text{ and } d.$$

The phase variable  $\varphi$  has the form  $\varphi_j = \mu_j x + \nu_j y + \omega_j t + \varphi_{j,0}$ ,  $j = 1, 2$ . The solution travels as the Zaitsev solution with constant speed in  $x$ -direction.

**REMARK 3.1.** *The standard 4th order Runge-Kutta scheme did not converge for any of the studied examples for the used time steps. The reason is that the Fourier multiplier  $-i/k_x$  imposes very strong stability restrictions on the scheme.*

### 3.2. Numerical solution of Cauchy problems for the KP I equation.

*Zaitsev solution.* We first study the case of the Zaitsev solution (3.3) with  $\alpha = 1$  and  $\beta = 0.5$ . Notice that this solution is unstable against small perturbations as shown numerically in [?], but that it can be propagated with the expected numerical precision by the used codes. As initial data we take the solution centered at  $-L_x/2$  (we use  $L_x = L_y = 5$ ) and propagate it until it reaches  $L_x/2$ . The computation is carried out with  $2^{11} \times 2^9$  points for  $(x, y) \in [-5\pi, 5\pi] \times [-5\pi, 5\pi]$  and  $t \leq 1$ . The decrease of the numerical error is shown in Fig. 3.1 in dependence of the time step and in dependence of the CPU time. A linear regression analysis in a double logarithmic plot ( $\log_{10} \Delta_2 = -a \log_{10} N_t + b$ ) is presented in Fig. 3.1, where we can see that all schemes show a fourth order behavior: we find  $a = 4.32$  for the Integrating Factor method,  $a = 4.38$  for DCRK method,  $a = 3.93$  for Krogstad's ETD scheme,  $a = 4$  for the Cox-Matthews scheme, and  $a = 3.98$  for the Hochbruck-Ostermann scheme.

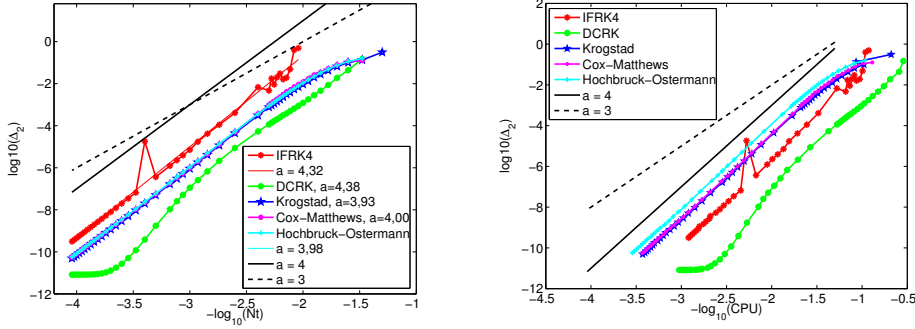


FIG. 3.1. Normalized  $L_2$  norm of the numerical error in the solution to the KP I equation with initial data given by the Zaitsev solution for several numerical methods, as a function of  $N_t$  (left) and as a function of CPU time (right).

In this context the DCRK method performs best, followed by the ETD schemes that have almost identical performance (though the Hochbruck-Osternmann method uses more internal stages and thus more CPU time in Fig. 3.1). It can also be seen that the various schemes do not show the phenomenon of order reduction as discussed in [?], which implies that the Zaitsev solution tests the codes in a non-stiff regime of the KP I equation.

*Small dispersion limit for KP I.* To study KP solutions in the limit of small dispersion ( $\epsilon \rightarrow 0$ ), we consider Schwartzian initial data satisfying the constraint (3.2). As in [?] we consider data of the form

$$u_0(x, y) = -\partial_x \text{sech}^2(R) \quad \text{where } R = \sqrt{x^2 + y^2}. \quad (3.6)$$

By numerically solving the dispersionless KP equation (put  $\epsilon = 0$  in (1.1)), we determine the critical time of the appearance of a gradient catastrophe by the breaking of the code, see [?]. To study dispersive shocks, we run the KP codes for some time larger than this critical time. The solution can be seen in Fig. 3.2. It develops tails with algebraic fall off towards infinity. The wave fronts steepen on both sides of the origin. In the regions of strong gradients, rapid modulated oscillations appear. For a detailed discussion, see [?].

The computation is carried out with  $2^{11} \times 2^9$  points for  $(x, y) \in [-5\pi, 5\pi] \times [-5\pi, 5\pi]$ ,  $\epsilon = 0.1$  and  $t \leq 0.4$ . As a reference solution, we consider the solution calculated with the Hochbruck-Osternmann method with  $N_t = 5000$  time steps. The normalized  $L_2$  norm of the difference between this reference solution and the numerical solution is shown in Fig. 3.3 in dependence on the time step with a regression analysis and in dependence on the CPU time. Here we can see clearly the phenomenon of order reduction established analytically for parabolic systems by Hochbruck and Osternmann [?]. In the stiff regime (here up to errors of order  $10^{-4}$ ) DCRK does not converge, the Integrating Factor method shows only first order behaviour (as predicted in [?]), the IRK4 scheme shows second order convergence, and ETD methods perform best. This implies that the Cox-Matthews and Krogstad method with similar performance are the most economic for the stiff regime of the KP I equation, which gives the precision one is typically interested in in this context. For higher precisions we find  $a = 1.87$

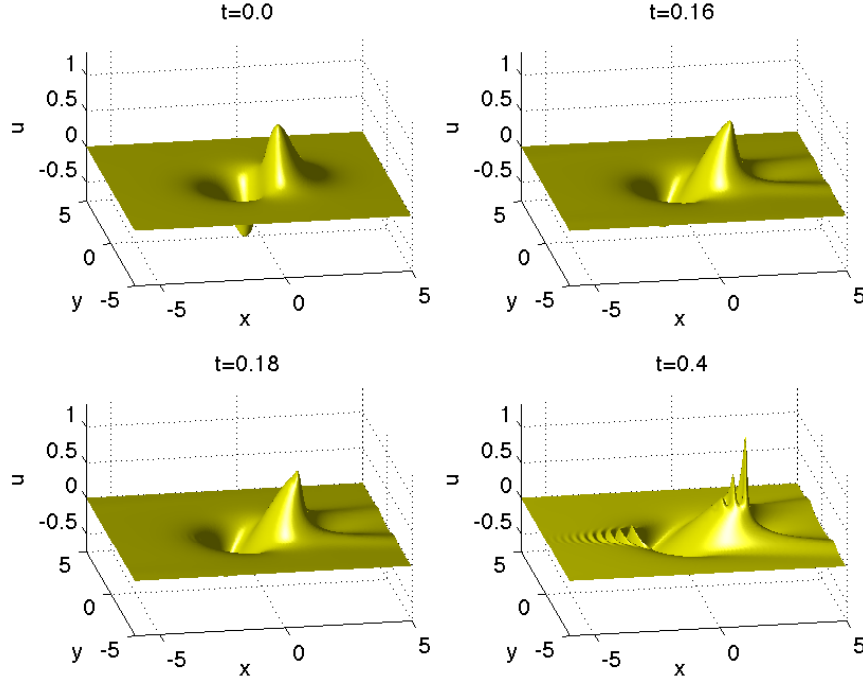


FIG. 3.2. Solution to the KP I equation for the initial data  $u_0 = -\partial_x \text{sech}^2(R)$  where  $R = \sqrt{x^2 + y^2}$  for several values of  $t$ .

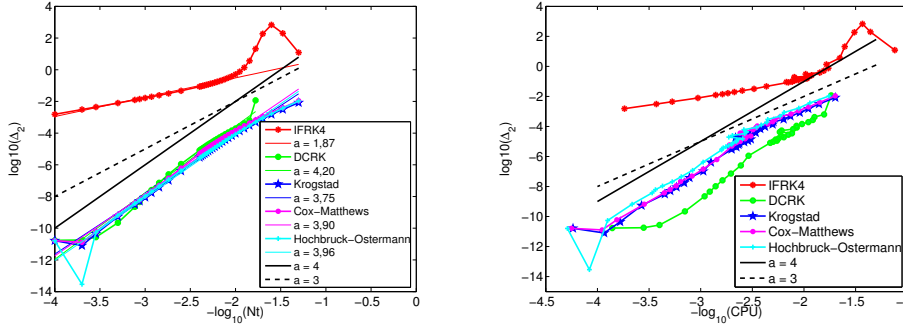


FIG. 3.3. Normalized  $L_2$  norm of the numerical error for the solution shown in Fig. 3.2 for several numerical methods, as a function of  $N_t$  (left) and as a function of CPU time (right).

for the Integrating Factor method,  $a = 4.20$  for DCRK,  $a = 4.03$  for IRK4,  $a = 3.75$  for Krogstad's ETD scheme,  $a = 3.90$  for the Cox-Matthews scheme, and  $a = 3.96$  for the Hochbruck-Ostermann scheme.

To study empirically the phenomenon of order reduction in exponential integrators, and to observe the transition from a stiff to a non stiff regime we study the ETD schemes in more detail in Fig. 3.4. This is indicated by the fact that ETD schemes are

only of order three in this stiff region instead of order four. It appears that all schemes

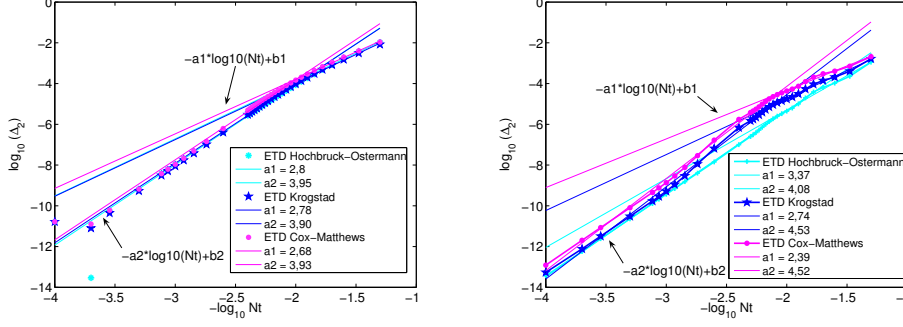


FIG. 3.4. Phenomenon of order reduction in exponential integrators for KP I and KP II respectively in the small dispersion limit, ETD schemes of Fig. 3.3 (left) and of Fig. 3.7 (right).

show a slight order reduction though this is not the case for the Hochbruck-Ostermann method in the parabolic case.

### 3.3. Numerical solution of Cauchy problems for the KP II equation.

*Doubly periodic solution of KP II.* The computation for the doubly periodic solution to KP II is carried out with  $2^8 \times 2^8$  points for  $(x, y) \in [-5\pi, 5\pi] \times [-5\pi, 5\pi]$  and  $t \leq 1$  with the parameters  $b = 1$ ,  $\lambda = 0.15$ ,  $b\lambda^2 + d = -1$ ,  $\mu_1 = \mu_2 = 0.25$ ,  $\nu_1 = -\nu_2 = 0.25269207053125$ ,  $\omega_1 = \omega_2 = -1.5429032317052$ , and  $\varphi_{1,0} = \varphi_{2,0} = 0$ . The decrease of the numerical error is shown in Fig. 3.5 in dependence of  $N_t$  and in dependence on CPU time. From a linear regression analysis in a double logarithmic

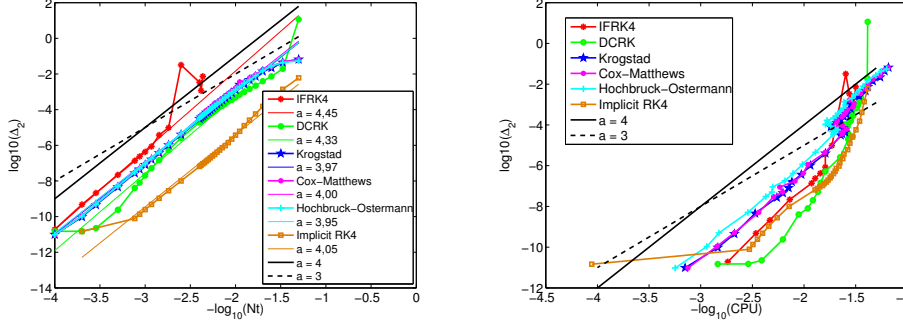


FIG. 3.5. Normalized  $L_2$  norm of the numerical error for the time evolution of the doubly periodic solution to the KP II equation for several numerical methods, as a function of  $N_t$  (left) and as a function of CPU time (right).

plot we can see that all schemes are fourth order: one finds  $a = 4.45$  for the Integrating Factor method,  $a = 4.33$  for DCRK,  $a = 3.97$  for Krogstad's ETD scheme,  $a = 4$  for the Cox-Matthews scheme, and  $a = 3.95$  for the Hochbruck-Ostermann scheme. As for the Zaitsev solution, DCRK performs best followed by the ETD schemes. We thus

confirm Driscoll's results in [?] on the efficiency of his method for this example. The absence of order reductions indicates again that the exact solution tests the equation in a non-stiff regime. IRK4 is competitive for larger time steps in this case since only very few iterations (1-3) are needed.

*Small dispersion limit for KP II.* We consider the same initial data and the same methods as for KP I. In Fig. 3.6 the time evolution of these data can be seen. The solution develops tails this time in negative  $x$ -direction. The steepening of the wave fronts happens at essentially the same time, but the gradients are stronger in the vicinity of the tails (see [?]). This is also where the stronger oscillations appear.

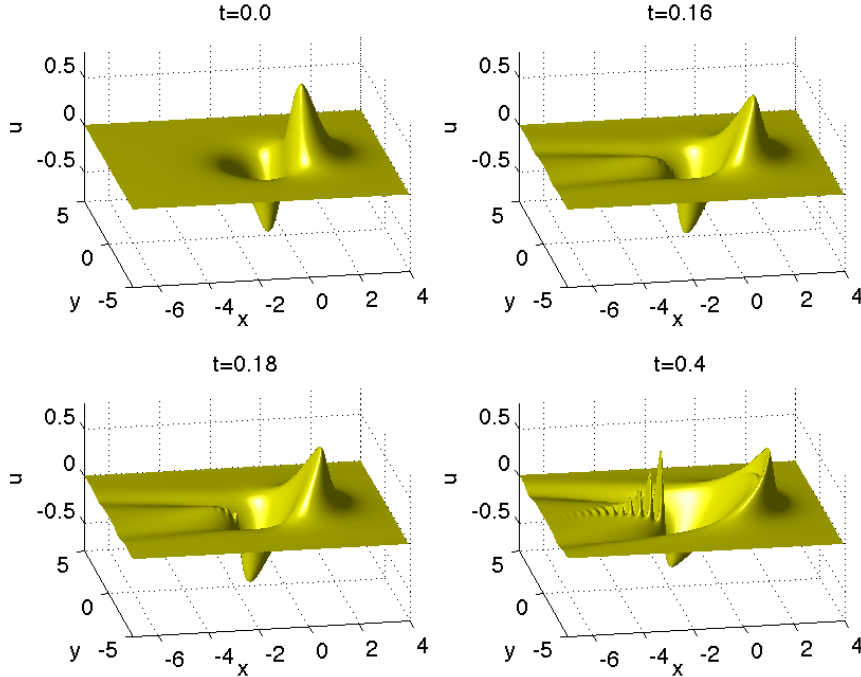


FIG. 3.6. Solution to the KP II equation for the initial data  $u_0 = -\partial_x \text{sech}^2(R)$  where  $R = \sqrt{x^2 + y^2}$  for several values of  $t$ .

The computation is carried out with  $2^{11} \times 2^9$  points for  $(x, y) \in [-5\pi, 5\pi] \times [-5\pi, 5\pi]$ ,  $\epsilon = 0.1$  and  $t \leq 0.4$ . As a reference solution, we consider the solution calculated with the Hochbruck-Ostermann method with  $N_t = 5000$  time steps. The dependence of the normalized  $L_2$  norm of the difference between this reference solution and the numerical solution on  $N_t$  and on CPU time is shown in Fig. 3.7. We obtain similar results as in the small dispersion limit of KP I: for typical accuracies one is interested in in this context, DCRK does not converge, the Integrating Factor method shows only a first order behavior, the IRK4 method is of second order, and the ETD methods perform best. In the non-stiff regime we find  $a = 1.06$  for the Integrating Factor method,  $a = 4.42$  for DCRK,  $a = 4.33$  for IRK4,  $a = 4.15$  for Krogstad's ETD scheme,  $a = 4.07$  for the Cox-Matthews scheme, and  $a = 3.99$  for the Hochbruck-Ostermann scheme. Once again, we study empirically the phenomenon of order reduction in exponential integrators, and observe a transition from a stiff to

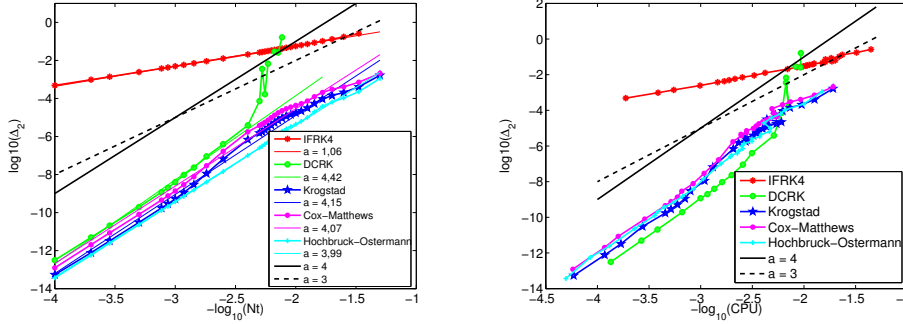


FIG. 3.7. Normalized  $L_2$  norm of the numerical error for the solution in Fig. 3.6 for several numerical methods as a function of  $N_t$  (left) and as a function of CPU time (right).

a non stiff region (Fig. 3.3), indicated by the fact that ETD schemes are only of order three in this stiff region instead of of order four.

**4. Davey-Stewartson equation.** In this section we perform a similar study as for KP of the efficiency of fourth methods in solving Cauchy problems for the DS II equations. We first review some analytic facts about the focusing and defocusing DS II equations which are of importance in this context. We compare the performance of the codes for a typical example in the small dispersion limit.

**4.1. Analytic properties of the DS equations.** For a review see for instance the book by Sulem and Sulem [?]. We will study here only the DS II equations ( $\alpha = \beta = 1$  in eq. (1.2)) since the elliptic operator for  $\Phi$  can be inverted by imposing simple boundary conditions. For a hyperbolic operator acting on  $\Phi$ , boundary conditions for wave equations have to be used.

We will consider the equations again on  $\mathbb{T}^2 \times \mathbb{R}$ . Due to the ellipticity of the operator in the equation for  $\Phi$ , it can be inverted in Fourier space in standard manner by imposing periodic boundary conditions on  $\Phi$  as well. As before this case contains Schwartzian functions that are periodic for numerical purposes. Notice that solutions to the DS equations for Schwartzian initial data stay in this space at least for finite time in contrast to the KP case. Using Fourier transformations  $\Phi$  can be eliminated from the first equation by a transformation of the second equation in (1.2) and an inverse transformation. With (2.5) we have

$$\Phi = -2\mathcal{F}^{-1} \left[ \frac{k_x^2}{k_x^2 + k_y^2} \mathcal{F} [|u|^2] \right],$$

which leads in (1.2) as for KP to a nonlocal equation with a Fourier multiplier. This implies that the DS equation requires an additional computational cost of 2 two-dimensional FFT per intermediate time step, thus doubling the cost with respect to the standard 2d NLS equation. Notice that from a numerical point of view the same applies to the elliptic-elliptic DS equation that is not integrable. Our experiments indicate that except for the additional FFT mentioned above, the numerical treatment of the 2d and higher dimensional NLS is analogous to the DS II case studied here. The restriction to this case is entirely due to the fact that one can hope for an asymptotic

description of the small dispersion limit in the integrable case. Thus we study initial data of the form  $u_0(x, y) = a(x, y) \exp(ib(x, y)/\epsilon)$  with  $a, b \in \mathbb{R}$ , i.e., the semi-classical limit well known from the Schrödinger equation. Here we discuss only real initial data for convenience.

It is known that DS solutions can have blowup. Results by Sung [?] establish global existence in time for initial data  $\psi_0 \in L_p$ ,  $1 \leq p < 2$  with a Fourier transform  $\mathcal{F}[\psi_0] \in L_1 \cap L_\infty$  subject to the smallness condition

$$\|\mathcal{F}[\psi_0]\|_{L_1} \|\mathcal{F}[\psi_0]\|_{L_\infty} < \frac{\pi^3}{2} \left( \frac{\sqrt{5}-1}{2} \right)^2 \quad (4.1)$$

in the focusing case. There is no such condition in the defocusing case. Notice that condition (4.1) has been established for the DS II equation with  $\epsilon = 1$ . The coordinate change  $x' = x/\epsilon$ ,  $t' = t/\epsilon$  transforms the DS equation (1.2) to this standard form. This implies for the initial data  $u_0 = \exp(-x^2 - \eta y^2)$  we study for the small dispersion limit of the focusing DS II system in this paper that condition (4.1) takes the form

$$\frac{1}{\epsilon^2 \eta} \leq \frac{1}{8} \left( \frac{\sqrt{5}-1}{2} \right)^2 \sim 0.0477.$$

This condition is not satisfied for the values of  $\epsilon$  and  $\eta$  we use here. Nonetheless we do not observe any indication of blowup on the shown timescales. One of the reasons is that the rescaling with  $\epsilon$  above also rescales the critical time for blowup by a factor  $1/\epsilon$ . In addition it is expected that the dispersionless equations will for generic initial data have a gradient catastrophe at some time  $t_c < \infty$ , and that the dispersion will regularize the solution for small times  $t > t_c > 0$ . However there are no analytic results in this context.

The complete integrability of the DS II equation implies again the existence of explicit solutions. Multi-soliton solutions will be as in the KP case localized in one spatial direction and infinitely extended in another, the lump solution is localized in two spatial directions, but with an algebraic fall off towards infinity. Thus these are again not convenient to test codes based on Fourier methods as in the KP case. Since the study of the small dispersion limit below indicates that the time steps have to be chosen sufficiently small for accuracy reasons such that in contrast to KP no order reduction observed, we will not study any exact solutions here.

**4.2. Small dispersion limit for DS II in the defocusing case.** We consider initial data  $u_0$  of the form

$$u_0(x, y) = e^{-R^2}, \text{ where } R = \sqrt{x^2 + \eta y^2} \text{ with } \eta = 1 \quad (4.2)$$

and use the same methods as before together with time splitting methods of order 2 and one of order 4, as explained in section 2.4. The defocusing effect of the defocusing DS II equation for these initial data can be seen in Fig. 4.1, where  $|u|^2$  is shown for several values of  $t$ . The compression of the initial pulse into some almost pyramidal shape leads to a steepening on the 4 sides parallel to the coordinate axes and to oscillations in these regions.

The computations are carried out with  $2^{10} \times 2^{10}$  points for  $(x, y) \in [-5\pi, 5\pi] \times [-5\pi, 5\pi]$ ,  $\epsilon = 0.1$  and  $t \leq 0.8$ . To determine a reference solution, we compute solutions with 6000 time steps with the ETD, the DCRK and the IF schemes and take



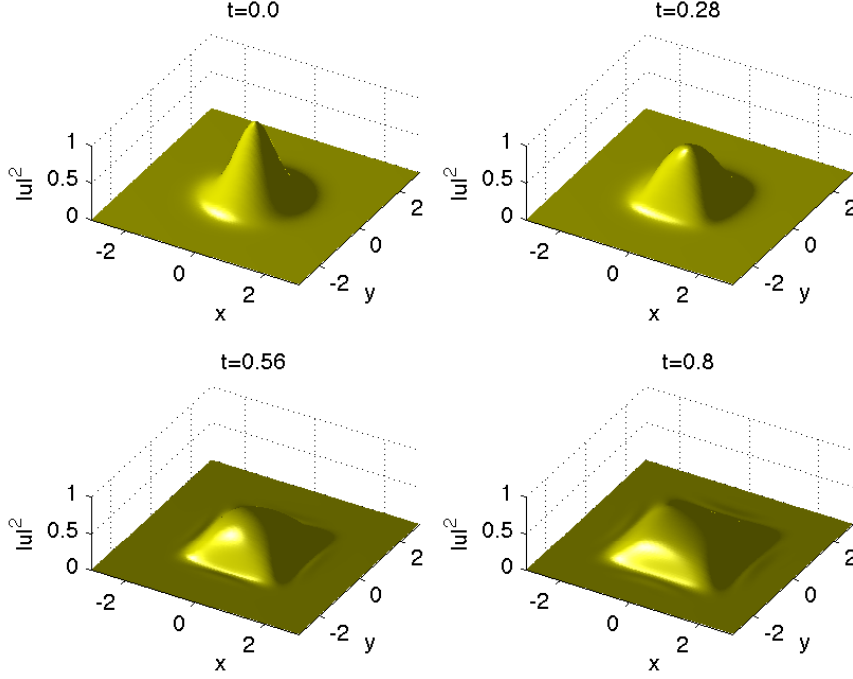


FIG. 4.1. Solution to the defocusing DS II equation for the initial data  $u_0 = \exp(-R^2)$  where  $R = \sqrt{x^2 + y^2}$  and  $\epsilon = 0.1$  for several values of  $t$ .

the arithmetic mean. The dependence of the normalized  $L_2$  norm of the difference of the numerical solutions with respect to this reference solution on  $N_t$  and on CPU time is shown in Fig. 4.2. A linear regression shows that all fourth order schemes show a

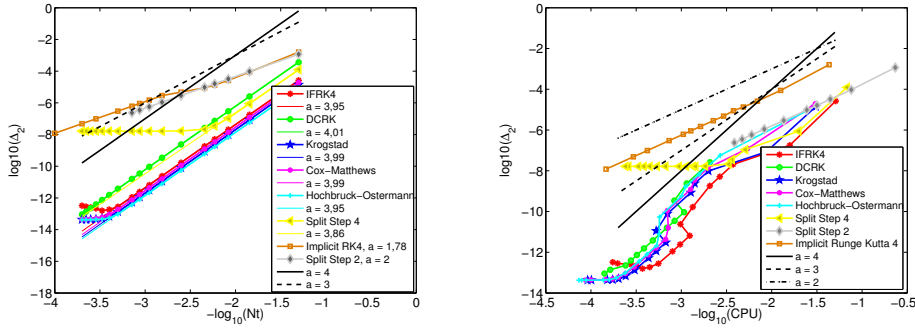


FIG. 4.2. Normalized  $L_2$  norm of the numerical error for several numerical methods for the situation shown in Fig. 4.1 as a function of  $N_t$  (left) and of CPU time (right).

fourth order behavior except for IRK4 ( $a = 1.78$ ), as is obvious from the straight lines with slope  $a = 3.95$  for the Integrating Factor method,  $a = 4.01$  for DCRK,  $a = 3.99$

for Krogstad's ETD scheme,  $a = 3.99$  for the Cox-Matthews scheme,  $a = 3.95$  for the Hochbruck-Ostermann scheme, and  $a = 3.86$  for the time splitting method. The second order splitting scheme shows the expected convergence rate and performs very well for lower precision. For smaller time steps, the advantage of the fourth order schemes is more pronounced. Apparently the system is 'stiff' for the IRK4 scheme since it only shows second order behavior. Notice that the time splitting scheme reaches its maximal precision around  $10^{-8}$ , a behavior which was already noticed in [?] for the study of the Nonlinear Schrödinger equation in the small dispersion limit. It appears that this behavior is due to resonances of errors of the split equations, but the identification of the precise reason will be the subject of further research. The same effect is observed for second order splitting for smaller time steps than shown in Fig. 4.2. However, both schemes work very well at the precisions in which one is normally interested in. We mainly include a second order scheme here because of the additional computational cost due to the function  $\Phi$  in the DS system. This could make a second order scheme competitive in terms of CPU time because of the lower number of FFT used per time step. It can be seen in Fig. 4.2 that this is not the case. We conclude that the ETD schemes perform best in this context.

**4.3. Small dispersion limit for the focusing DS II equation.** For the focusing DS II in the small dispersion limit we consider initial data of the form (4.2) with  $\eta = 0.1$  and the same methods as before. The focusing effect of the equation can be clearly recognized in Fig. 4.3. The initial peak grows until a breakup into a pattern of smaller peaks occurs.

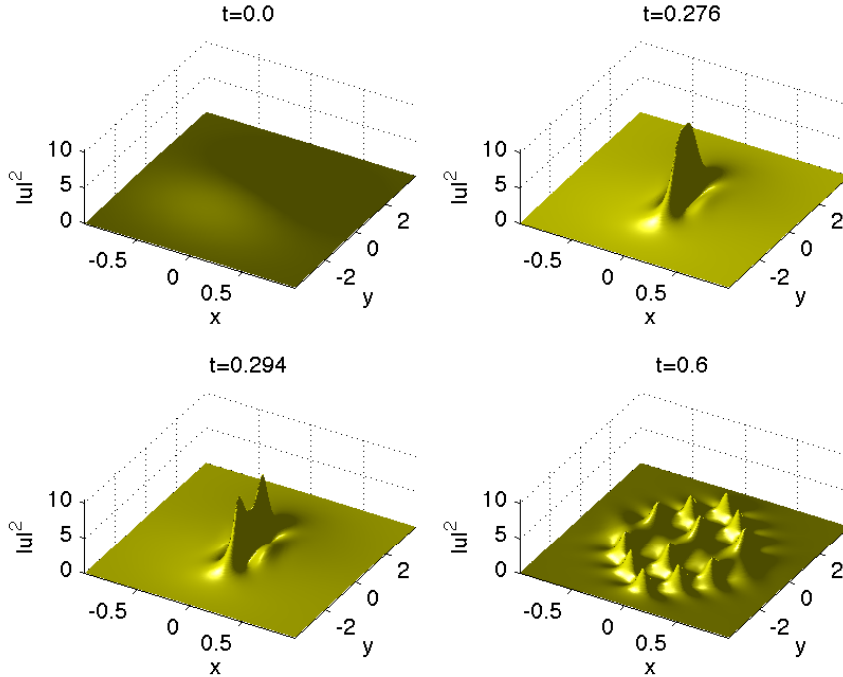


FIG. 4.3. *Solution to the focusing DS II equation for the initial data  $u_0 = \exp(-R^2)$  where  $R = \sqrt{x^2 + \eta y^2}$ ,  $\eta = 0.1$  and  $\epsilon = 0.1$  for several values of  $t$ .*

It is crucial to provide sufficient spatial resolution for the central peak. As for the 1+1-dimensional focusing NLS discussed in [?], the modulational instability of the focusing DS II leads to numerical problems if there is no sufficient resolution for the maximum. In [?] a resolution of  $2^{13}$  modes was necessary for initial data  $e^{-x^2}$  and  $\epsilon = 0.1$  for the focusing NLS in 1 + 1 dimensions. The possibility of blowup in DS requires at least the same resolution despite some regularizing effect of the nonlocality  $\Phi$ . With the computers we could access, a systematic study of time integration schemes with a resolution of  $2^{13} \times 2^{13}$  was not possible in Matlab. Thus we settled for initial data close to the one-dimensional case, which allowed for a lower resolution, see the next section for the Fourier coefficients. The computation is carried out with  $2^{12} \times 2^{11}$  points for  $(x, y) \in [-5\pi, 5\pi] \times [-5\pi, 5\pi]$ ,  $\epsilon = 0.1$  and  $t \leq 0.6$ . To determine a reference solution, we compute solutions with 6000 time steps with the ETD, the DCRK and the IF schemes and take the arithmetic mean. The dependence of the normalized  $L_2$  norm of the difference of the numerical solutions with respect to this reference solution on  $N_t$  and on CPU time is shown in Fig. 4.4. All schemes

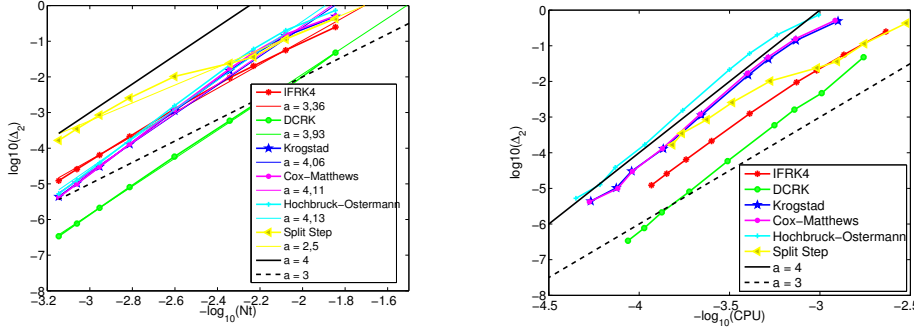


FIG. 4.4. Normalized  $L_2$  norm of the numerical error for the example of Fig. 4.3 for several numerical methods as a function of  $N_t$  (left) and of CPU time (right).

except the time splitting scheme show a fourth order behavior, as can be seen from the straight lines with slope  $a = 3.36$  for the Integrating Factor method,  $a = 3.93$  for DCRK,  $a = 4.06$  for Krogstad's ETD scheme,  $a = 4.11$  for the Cox-Matthews scheme,  $a = 4.13$  for the Hochbruck-Ostermann scheme, and  $a = 2.5$  for the fourth order time splitting method. We conclude that in this context DCRK performs best, followed by the ETD schemes. We do not present results for the IRK4 scheme here since it was computationally too expensive.

**5. Numerical conservation of the  $L_2$  norm.** The complete integrability of the KP and the DS equations implies the existence of many or infinitely many conserved quantities (depending on the function spaces for which the solutions are defined). It can be easily checked that the  $L_1$  norm and the  $L_2$  norm of the solution are conserved as well as the energy. We do not use here symplectic integrators that take advantage of the Hamiltonian structure of the equations. Such integrators of fourth order will be always implicit which will be in general computationally too expensive for the studied equations as the experiment with the implicit IRK4 scheme showed. Moreover it was shown in [?] that fourth order exponential integrators clearly outperform second order symplectic integrators for the NLS equation.

The fact that the conservation of  $L_2$  norm and energy is not implemented in the code allows to use the ‘numerical conservation’ of these quantities during the computation or the lack thereof to test the quality of the code. We will study in this section for the previous examples to which extent this leads to a quantitative indicator of numerical errors. Note that due to the non-locality of the studied PDEs (1.1) and (1.2), the energies both for KP,

$$E[u(t)] := \frac{1}{2} \int_{\mathbb{T}^2} (\partial_x u(t, x, y))^2 - \lambda (\partial_x^{-1} \partial_y u(t, x, y))^2 - 2\epsilon^2 u^3(t, x, y) dx dy,$$

and for DS II,

$$E[u(t)] := \frac{1}{2} \int_{\mathbb{T}^2} \left[ \epsilon^2 |\partial_x u(t, x, y)|^2 - \epsilon^2 |\partial_y u(t, x, y)|^2 - \rho \left( |u(t, x, y)|^4 - \frac{1}{2} (\Phi(t, x, y)^2 + (\partial_x^{-1} \partial_y \Phi(t, x, y))^2) \right) \right] dx dy,$$

contain anti-derivatives with respect to  $x$ . Since the latter are computed with Fourier methods, i.e., via division by  $k_x$  in Fourier space, this computation is in itself numerically problematic and could indicate problems not present in the numerical solution of the Cauchy problem. Therefore we trace here only the  $L_2$  norm  $\int_{\mathbb{T}^2} |u(t, x, y)|^2 dx dy$ , where these problems do not appear. In the plots we show the variable *test* defined as  $test = M(t)/M(0) - 1$ , where  $M(t)$  is the numerically computed  $L_2$  norm in dependence of time.

Notice that numerical conservation of the  $L_2$  norm can be only taken as an indication of the quality of the numerics if there is sufficient spatial resolution. Therefore we will always present the Fourier coefficients for the final time step for the considered examples. No dealiasing techniques are used. We will discuss below the results for the small dispersion limit.

For the KP I example of Fig. 3.2 we get the Fourier coefficients at the final time and the mass conservation shown in Fig. 5.1. It can be seen that the Fourier coefficients decrease in  $k_x$ -direction to almost machine precision, whereas this is not fully achieved in  $k_y$ -direction. This is partly due to the necessity to allow extensive studies of the dependence on the time-stepping in finite computing time and thus to keep the spatial resolution low, and partly due to a Gibbs phenomenon mainly in  $k_y$ -direction due to the formation of the algebraic tails in Fig. 3.2. Mass conservation can be seen to be a viable indicator of the numerical accuracy by comparing with Fig. 3.3: in the range of accuracy in which one is typically interested ( $\sim 10^{-4}$ ), mass conservation overestimates the actual accuracy by roughly 2 orders of magnitude. It can be seen that it shows also at least a fourth order decrease.

The situation is very similar for the small dispersion example for KP II of Fig. 3.6 as can be seen in Fig. 5.2.

For the defocusing DS II equation and the example shown in Fig. 4.1, the Fourier coefficients decrease to machine precision despite the lower resolution than for KP. One reason for this is the absence of algebraic tails in the solution. The mass shows as for KP at least fourth order dependence on the time step and overestimates the numerical precision by roughly two orders of magnitude. This is not true for the splitting scheme for which mass conservation is no indication of the numerical precision at all. This seems to be due to the exact integration of the equations (2.7) into which DS is split (for one of them the  $L_2$  norm is constant). The found numerical mass does not appear to reflect the splitting error that is the reason for the numerical error here.

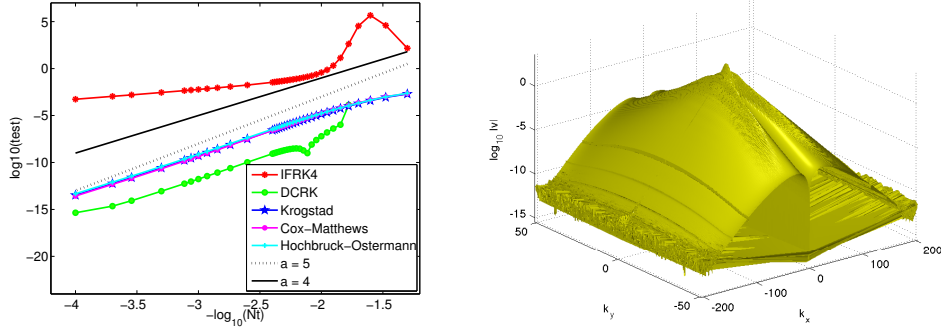


FIG. 5.1. Non-conservation of the numerically computed  $L_2$  norm of the solution to the problem considered in Fig. 3.3 in dependence on the time step (left) and the Fourier coefficients for the final time (right).

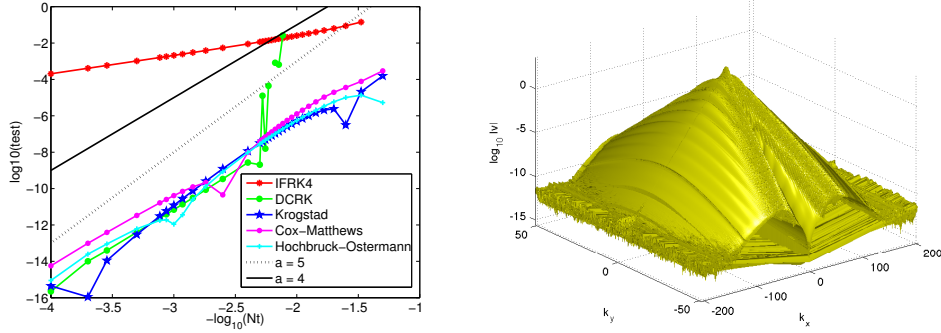


FIG. 5.2. Non-conservation of the numerically computed  $L_2$  norm of the solution to the problem considered in Fig. 3.7 in dependence on the time step (left) and the Fourier coefficients for the final time (right).

For the small dispersion example for the focusing DS II equation of Fig. 4.1 it can be seen in Fig. 5.4 that spatial resolution is almost achieved. There is a certain lack of resolution in the  $k_x$  direction which leads to the formation of some structure close to  $k_y = 0$ . This is related to the modulational instability of solutions to the focusing DS II equation. It will disappear for higher resolutions. Numerical conservation of the  $L_2$  norm of the solution overestimates numerical accuracy by 2-3 orders of magnitude for an error of the order of  $10^{-3}$ . Once more it cannot be used as an indicator for the numerical error in the splitting case, where it is almost independent of the time step. For the other cases numerical conservation of the  $L_2$  norm shows a dependence on  $N_t$  between fourth and fifth order. This indicates as for the NLS case in [?] that the numerical error has a divergence structure which leads to a higher order decrease of the  $L_2$  norm than for the actual error. This behavior is also present in the above examples, but less pronounced.

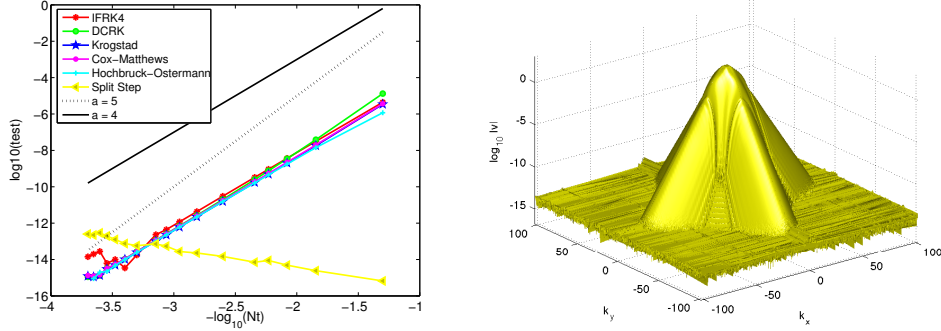


FIG. 5.3. Non-conservation of the numerically computed  $L_2$  norm of the solution to the problem considered in Fig. 4.2 in dependence on the time step (left) and the Fourier coefficients for the final time (right).

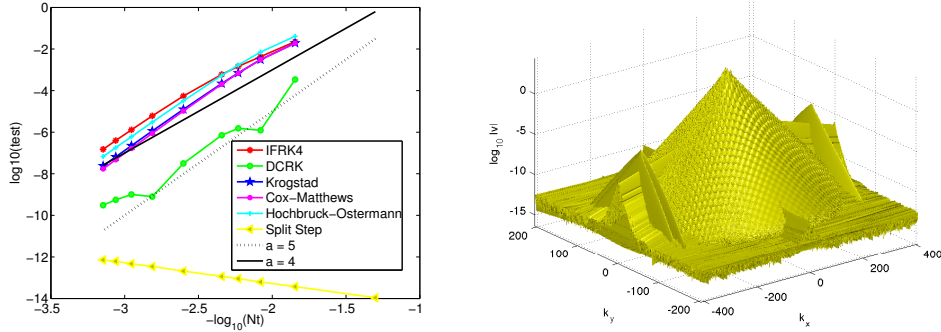


FIG. 5.4. Non-conservation of the numerically computed  $L_2$  norm of the solution to the problem considered in Fig. 4.4 in dependence on the time step (left) and the Fourier coefficients for the final time (right).

**6. Conclusion.** It was shown in this paper that fourth order time stepping schemes can be efficiently used for higher dimensional generalizations of the KdV and the NLS equations, where the stiffness of the system of ODEs obtained after spatial discretization can be a problem. Implicit schemes as IRK4 are computationally too expensive in the stiff regime, whereas standard explicit schemes as RK require for stability reasons too restrictive requirements on the time steps for the KP and DS equations. For these equations the non-localities in the PDEs lead to singular Fourier multipliers which make standard explicit schemes in practice unusable for stability reasons.

IMEX schemes do not converge in general for similar reason. Driscoll's composite RK variant is generally very efficient if the studied system is not too stiff, but fails to converge for strong stiffness. Exponential integrators do not have this problem. The order reduction phenomenon is a considerable problem for IF schemes in the stiff regime, but less so for ETD schemes. The Hochbruck-Osternann method performs

in general best, but the additional stage it requires is in practice not worth the effort in comparison with Krogstad's or Cox-Matthews' method. The computation of the  $\phi$ -functions in ETD is inexpensive for the studied problems since it has to be done only once.

Since stiffness is not the limiting factor for DS II, all schemes perform well in this context. But the modulational instability of the focusing case requires high spatial resolution we could not achieve in Matlab on the used computers for more general initial data. Thus the code will be parallelized to allow the use of higher spatial resolution without allocating too much memory per processor.